FISCHER-TROPSCH SLURRY PHASE PROCESS VARIATIONS TO UNDERSTAND WAX FORMATIONS: QUARTERLY REPORT, JULY 1, 1987-SEPTEMBER 30, 1987

MASSACHUSETTS INST. OF TECH., CAMBRIDGE

1987

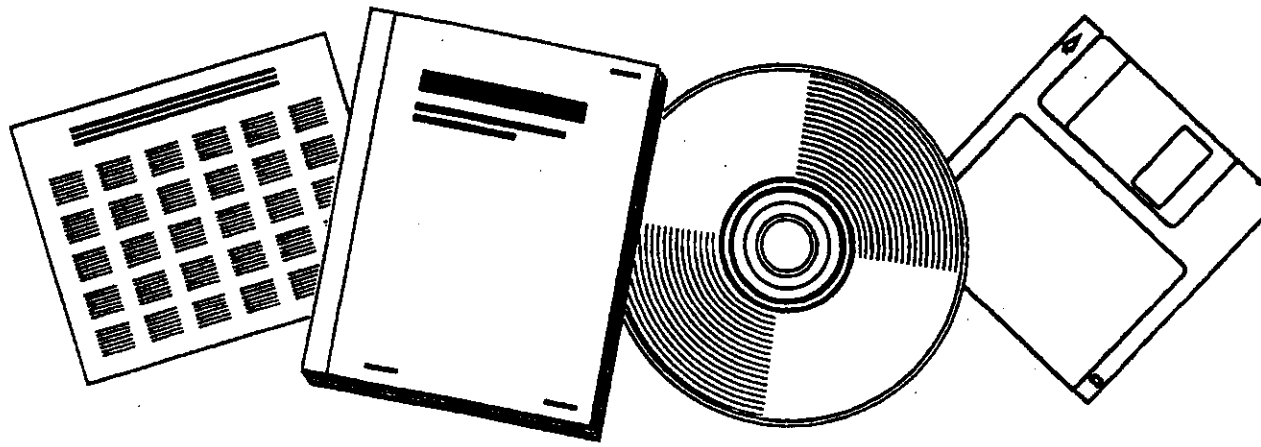

U.S. DEPARTMENT OF COMMERCE
National Technical Information Service

Fischer-Tropsch Slurry Phase Process Variations to Understand Wax Formations

Quarterly Report for Period July 1, 1987 to September 30, 1987

Report No.: DOE/PC80015-8

Contract No.: DE-AC22-85PC80015

by

Charles N. Satterfield

for

U.S. Department of Energy

Pittsburgh Energy Technology Center

P.O. Box 10940-MS 920-L

Pittsburgh, PA 15236

Attention: Swenam R. Lee, Project Manager

DOE/PC/80015--8

DE88 001855

ACKNOWLEDGEMENT

This work was sponsored by the Pittsburgh Energy Technology Center (PETC) of the United States Department of Energy (DOE). The author would like to express his appreciation to Mr. Swenam R. Lee at PETC, Project Manager, and Dr. John Shen at DOE-Washington, for their contributions to this project.

Table of Contents

		Page
I.	Preliminary Results from Ruhrchemie Catalyst	1
II.	Effect of Added CO_2 on the Fischer-Tropsch Synthesis	13

Summary

The performance of a sample of Ruhrchemie catalyst is compared in an approximate fashion to that of a PETC precipitated Fe catalyst, Mobil low wax and high wax catalysts, Sasol fixed bed catalyst and C-73 fused magnetite catalyst. Preliminary analysis of the results indicates that the Ruhrchemie catalyst has about one-third the activity of the other catalysts, and is much less active for the water gas shift. It shows a double α distribution, breaking at about C_7, $\alpha_1 = 0.68$ and $\alpha_2 = 0.85$. $C_{12}+$ formation was comparable to that from the PETC catalyst and the Mobil low wax catalyst, higher than that from C-73 and lower than that produced by Mobil high wax catalyst and in the Sasol fixed bed reactors. These above results are preliminary. Data are still being analyzed.

The effect of adding CO_2 during synthesis on a C-73 magnetite catalyst has been studied. CO_2 forms H_2O by the reverse water gas shift and the kinetics observed can be attributed to the H_2O formation. The effects on product selectivity also seem to be mostly attributable to the H_2O formed. These results are preliminary. Data are still being analyzed and other methods of correlation are being explored.

I. Preliminary Results from Ruhrchemie Catalyst

Summary

A series of 35 material balances was performed using a Ruhrchemie catalyst supplied to us by Ruhrchemie. Activity and selectivity were studied and are compared to literature values for several Fischer-Tropsch catalysts. A heating tape was used to bring the reactor head temperature closer to the slurry temperature with a resulting slight increase in syngas conversion. This report represents analysis of only about one-third of the material balances performed. The remaining runs are still being analyzed.

Introduction

The Ruhrchemie catalyst is a precipitated iron catalyst promoted with potassium. The catalyst was formerly used at SASOL in the fixed bed units operating between 220 and 250 C. Its composition as determined by Galbraith is given below.

Fe	47.30 weight %	Al	0.02 weight %
Cu	2.36	C	0.16
K	1.94	H	1.09
SiO_2	12.69	Ca	0.08

The balance (34.36%) is assumed to be oxygen in metal oxide forms. The composition, including the silica content falls in the range described by Anderson (1984). A sieve size of 170-270 mesh was used here.

Our plan is to compare the performance of this promoted precipitated catalyst to that of an unpromoted catalyst obtained from PETC. Both product distribution and catalyst activity will

be considered. This set of experiments also allows comparison with the large amount of data collected in our lab using C-73 fused magnetite.

Experimental

The catalyst was reduced in our reduction unit rather than in situ, so that we could determine the extent of reduction by weight loss. Because of its low density (~0.7g/cc), the catalyst was packed tightly into the unit and held snug with a glass wool plug. This is in contrast to our usual fluidized reduction of C-73. The catalyst was charged to the reactor and showed similar activity to catalyst reduced in situ in earlier experiments in this laboratory. The catalyst weight loss on reduction was about 10%, corresponding to about a 30-35% loss of oxygen. This is a somewhat milder reduction than the 40 to 60% mentioned in various literature sources. The catalyst was brought up to temperature slowly, then reactor temperature was varied between 230 and 265° C. Reactor pressure was typically 25 atm and flow was near 1.5 Nl/h/gFe. The feed composition for all material balances was 0.7 H_2/CO. Usage ratios varied from about 0.9 to 1.8. Returning to a given set of conditions periodically throughout the run indicated no loss in activity. At this time, only twelve material balances have been completely analyzed for selectivities (Table 1). Activity information for all runs has been calculated.

Results

I. Selectivity

A. A break in the Shultz-Flory diagram is observed at about C_7; α_1 has been calculated in the range C_3-C_7 and α_2 in the range C_{10}-C_{16}. The value of α_1 is 0.66 at 263°C and α_2 is 0.83 (Figure 1). Some Flory diagrams showed an apparent increase in mole fraction at about C_{10}, as shown in Figure 2. No good explanation for this behavior has suggested itself yet. It is possible that it is an artifact of the trapping procedures and temperatures.

B. Both α_1 and α_2 decrease as temperature increases (Figure 3). This agrees with Dry's report of SASOL data (1983). There may also be a slight decrease in chain-growth probability as conversion is increased (Figure 4), but the temperature effect appears more significant.

C. α-olefin/n-paraffin ratio is about 4 at C_5 and about 2 at C_{12}. At lower carbon numbers, olefin/paraffin ratio seems to increase linearly with temperature but at higher carbon numbers, less effect is noticed.

T, °C	C_5 ole/par	C_{12} ole/par
232	3.2	2.0
248	3.9	1.9
263	4.4	1.8

Olefin/paraffin ratio is independent of conversion. Essentially no β-olefins are produced, in contrast to the C-73 catalyst.

D. Methane production increases with temperature and is independent of conversion.

T, °C	CH_4 wt %
232	3.4
248	4.5
263	5.9

E. Selectivity to oxygenates is not dependent on temperature, but is decreased at higher conversions. The effects of temperature and conversion on methane and oxygenate selectivity and olefin/paraffin ratio are shown graphically in Figures 5 and 6.

F. Analysis of a wax sample drawn from the reactor after one week on stream showed a value of α_2 of 0.91 in the C_{21}-C_{26} range. In the same range, olefin to paraffin ratio was near 1.0. It should be noted that an equilibrium product distribution may not yet have been present in the wax for this carbon number range. Overhead product streams from later material balances showed olefin/paraffin ratios of about 1.3 in this range, but VLE problems may give misleading information for wax products.

G. The selectivity of the Ruhrchemie catalyst is comparable to a PETC catalyst promoted with 0.3 wt% potassium (Zarochak, 1987) and to a Mobil low-wax catalyst, class I-B (Kuo, 1983). A high-wax class I-B Mobil catalyst (Kuo, 1985) and the SASOL fixed-bed catalyst (Caldwell, 1980) both produce larger wax-fractions. The fused iron C-73 catalyst produces much less wax and about twice the methane of the Ruhrchemie catalyst. Table 2 compares the selectivity and activity of these catalysts, but these numbers should be treated cautiously. We have tried to find a set of operating conditions as nearly common as possible.

Values of α_1 and α_2 for the two Mobil catalyst compositions are approximated.

II. Activity

A. The Ruhrchemie catalyst appears to be significantly less active for syngas conversion that other precipitated or fused iron catalysts (Table 2). Even at a pressure of 25 atm, conversion of $CO+H_2$ is about half that on either Mobil catalyst or the PETC catalyst at about 15 atm. We have been unable thus far to obtain reliable data on the activity of the SASOL catalyst from the literature.

B. The water-gas shift activity of the Ruhrchmie catalyst is markedly lower than that of C-73 or the other catalysts. The reaction quotient for water-gas shift is $[CO_2][H_2]/[CO][H_2O]$; the value of this quotient for several catalysts is given in Table 2. Perhaps a more useful number, the extent of reaction of water-gas shift is about 60% for the Ruhrchemie catalyst at 248°C as compared to about 90% for C-73. Kuo (1985) suggests that low shift activity could lead to higher catalyst aging rates, due to low H_2/CO ratios in the reactor. It may be desirable to run this catalyst at a high H_2/CO feed ratio.

C. Reduction of this catalyst in situ gave similar activity to reduction followed by charging to the reactor. No complete analyses of liquid smaples from the in situ runs are available, so selectivity comparisons are difficult to attempt. Both Mobil and PETC advise catalyst pre-treatment in situ under syngas, rather than hydrogen. With this in mind, no further attempt will be made to reduce precipitated catalysts externally.

References

Anderson, R.B., The Fischer-Tropsch Synthesis, Academic Press, New York (1984), pp. 144-145.

Caldwell, L., "Selectivity in Fischer-Tropsch Synthesis," CSIR Report CENG 330, Pretoria (1980).

Dry, M.E., "The Sasol Fischer-Tropsch Processes," Appl. Ind. Cat. 2, 167 (1983).

Kuo, J.C.W., Slurry Fischer-Tropsch/Mobil Two Stage Process of Converting Syngas to High Octane Gasoline, Final Report, DOE/PC/30022-10 (DE84004411), 1983.

Kuo, J.C.W., Two-Stage Process for Conversion of Synthesis Gas to High Quality Transportation Fuels, Final Report, DOE/PC/60019-9 (1985).

Zarochak, M., M. McDonald and V. Rao, "Stability and Selectivity of Potassium Promoted Iron Catalyst in Slurry Fischer-Tropsch Synthesis," 12th Annual Conf. on Fuel Sciences, May 13-14, 1987, Palo Alto.

Table 1: Fully Analyzed Material Balances

Mat.Bal.	Temp., C	P, psig	Qo, l/min	CO+H2 %conv.
6	248	380	0.363	35.8
8	248	380	0.862	22
12	232	380	0.56	18.5
13	232	380	0.557	18.4
14	263	380	0.559	41.3
15	263	380	0.365	52.4
16	263	380	0.86	33.6
19	248	380	0.555	30.4
25	248	380	0.559	37.6
30	263	380	0.853	39.7
31	248	380	0.56	33.6
32	248	380	0.363	43.9

Table 2: Catalyst Comparison

	Ruhrchemie	PETC	Mobil low wax	Mobil high wax	SASOL fixed bed	C-73
Selectivity						
Methane	5.7	5.1	8.0	2.6	5.0	11.6
C2-C4	27.0	20.9	22.7	9.2	12.6	39.6
C5-C11	40.0	42.9	39.7	14.2	22.5	39.5
C12 +	27.3	31.1	29.6	70.5	56.0	9.3
alpha 1	0.68		0.85	0.79	0.87	
alpha 2	0.85		0.94	0.97	0.90	note a, below
gHC/Nm3 conv.	172		218	182		183
Activity						
mmol/min.gFe	0.49	1.3	1.3	1.5		0.37
act/atmH2	0.05					0.15
[CO2][H2]/[CO][H2O]	0.7	20.0		39.0		40.0
Conditions						
T, C	263	260	262	249	220-250	263
P, atm	25	13	15	15	25	8-15
Nl/h/gFe	2.0	2.4	2.1	2.4		1.0
CO+H2 conv.	33.6	72.2	84.3	86.3		56.0

[a] Values of α_1 and α_2 on C-73 vary somewhat with pressure, temperature and gas composition. Representative values of α_1 are 0.64 - 0.68; α_2 of 0.78 - 0.9.

Figure 1

RC3.16 Shulz-Flory Diagram

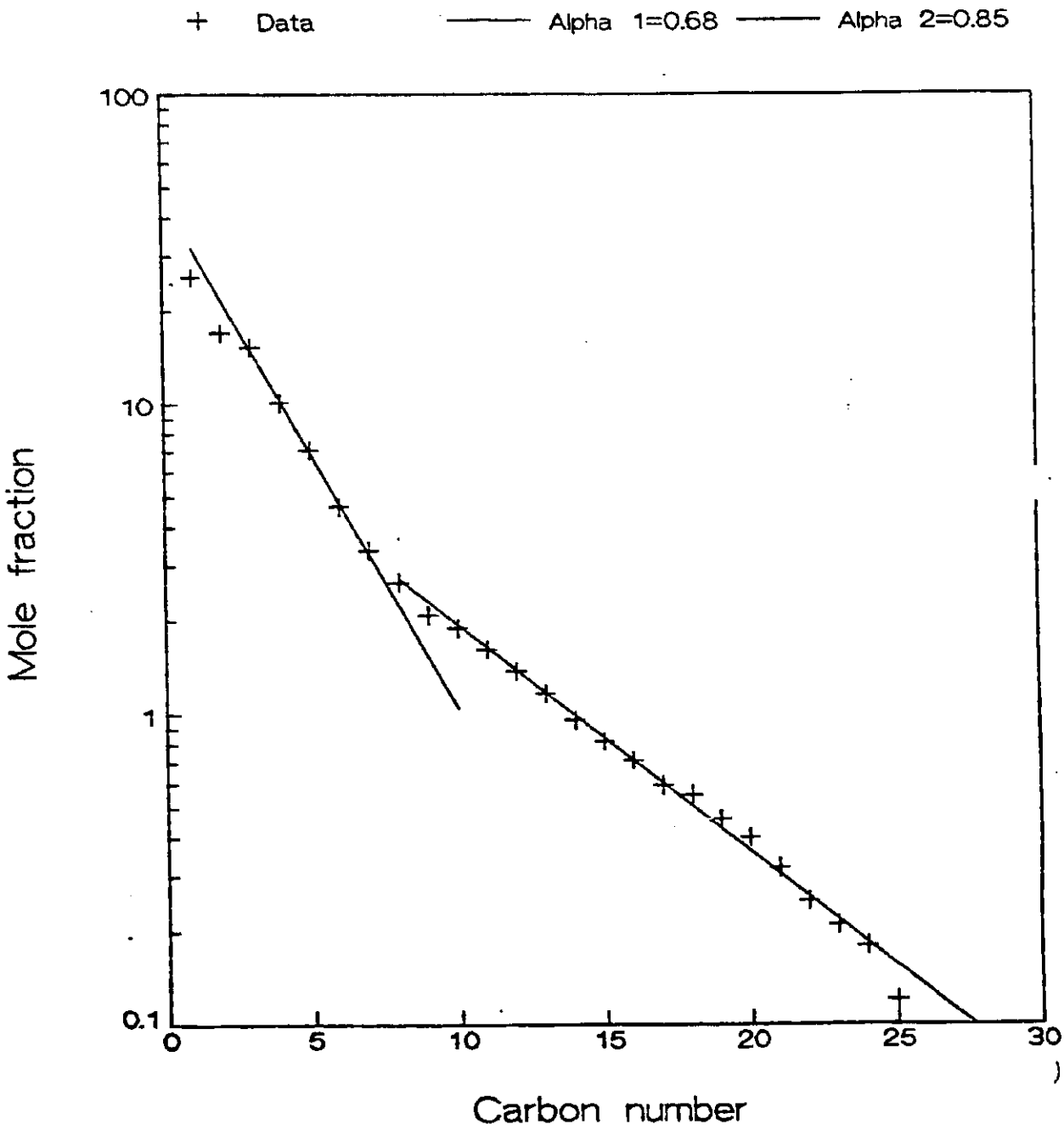

Figure 2

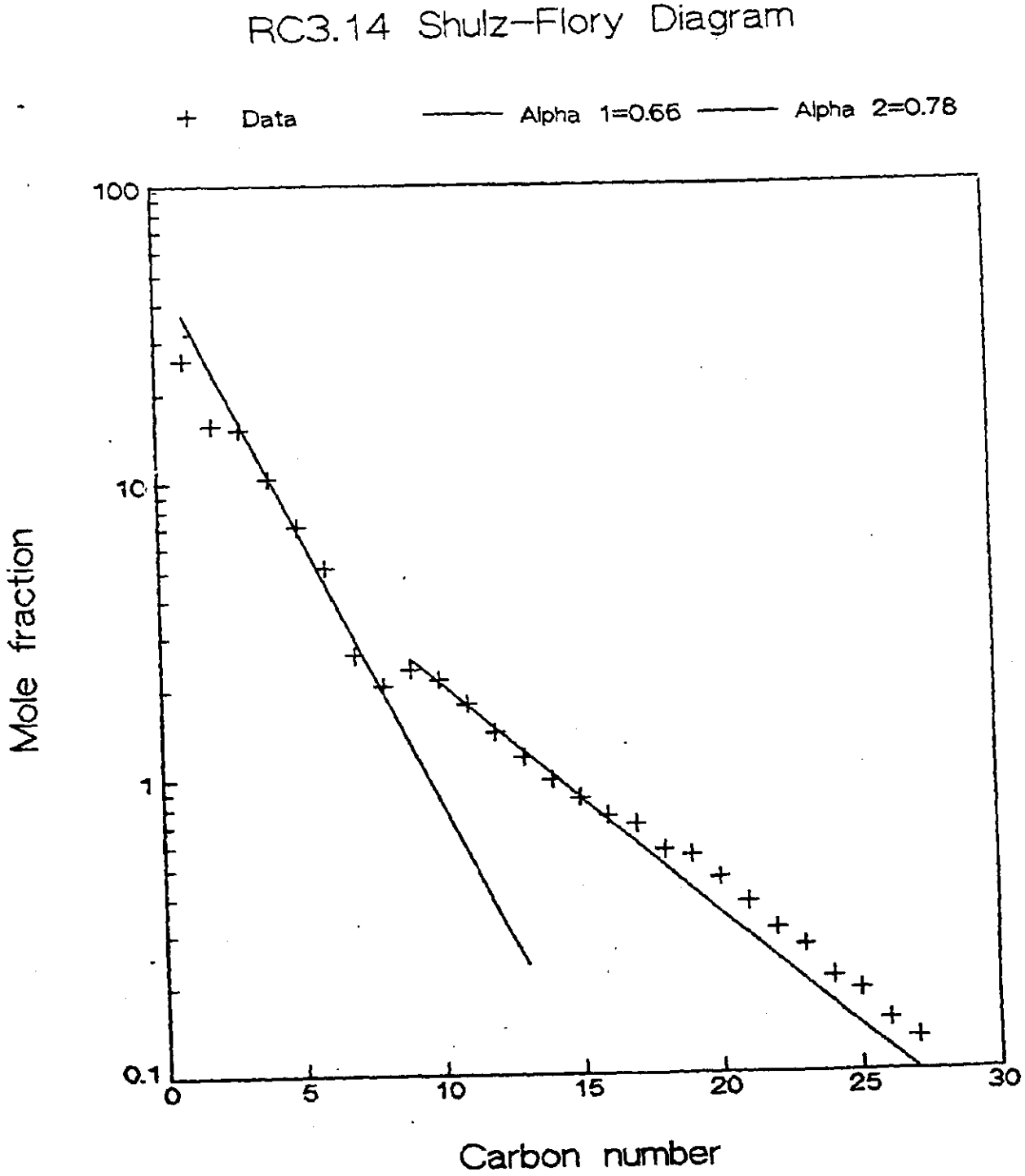
RC3.14 Shulz-Flory Diagram
+ Data
Alpha 1=0.66
Alpha 2=0.78
Mole fraction
100
10
1
0.1
0
5
10
15
20
25
30
Carbon number

Figure 3

Temperature Dependence of Alpha
Constant Space Velocity

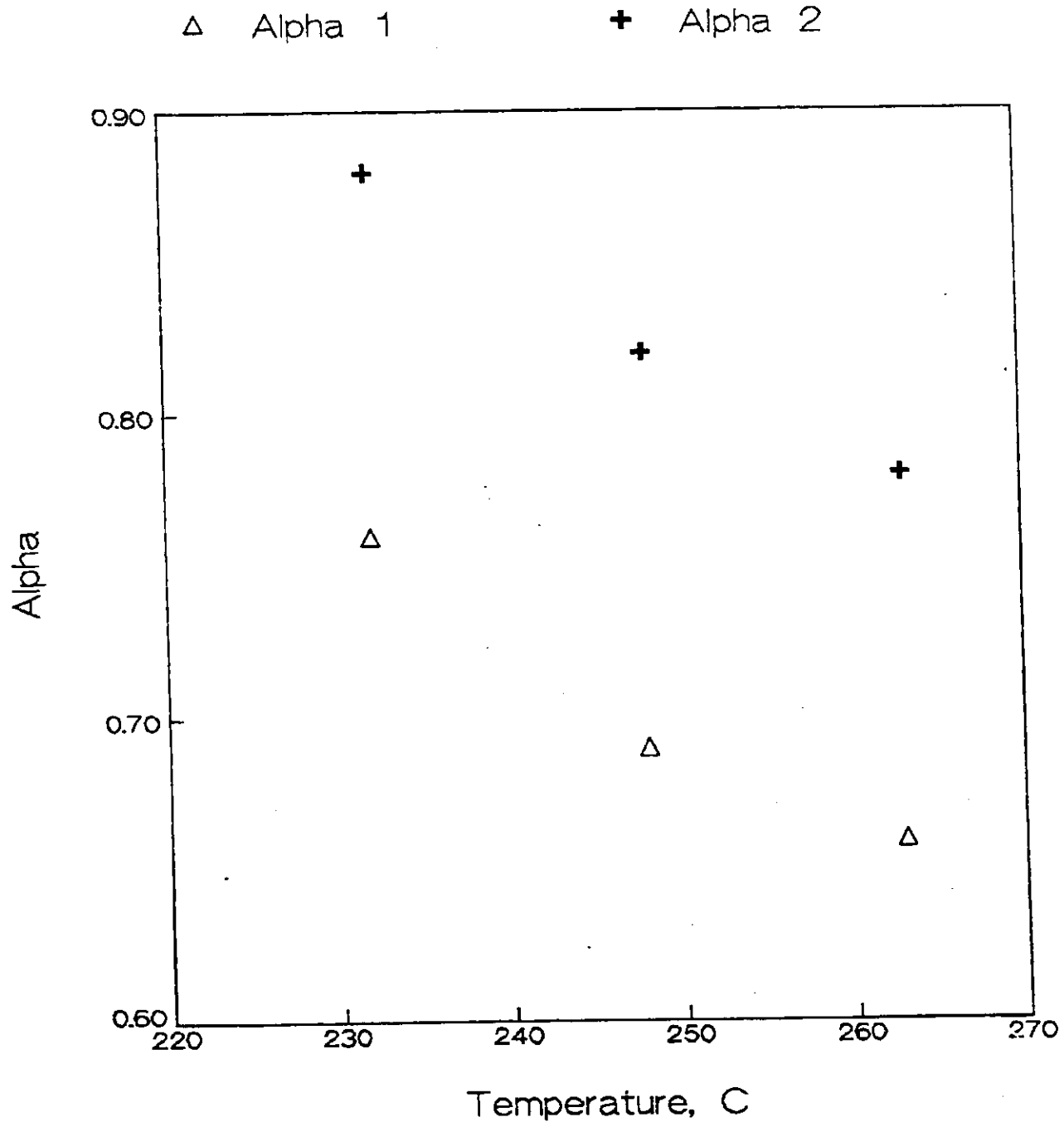

Figure 4

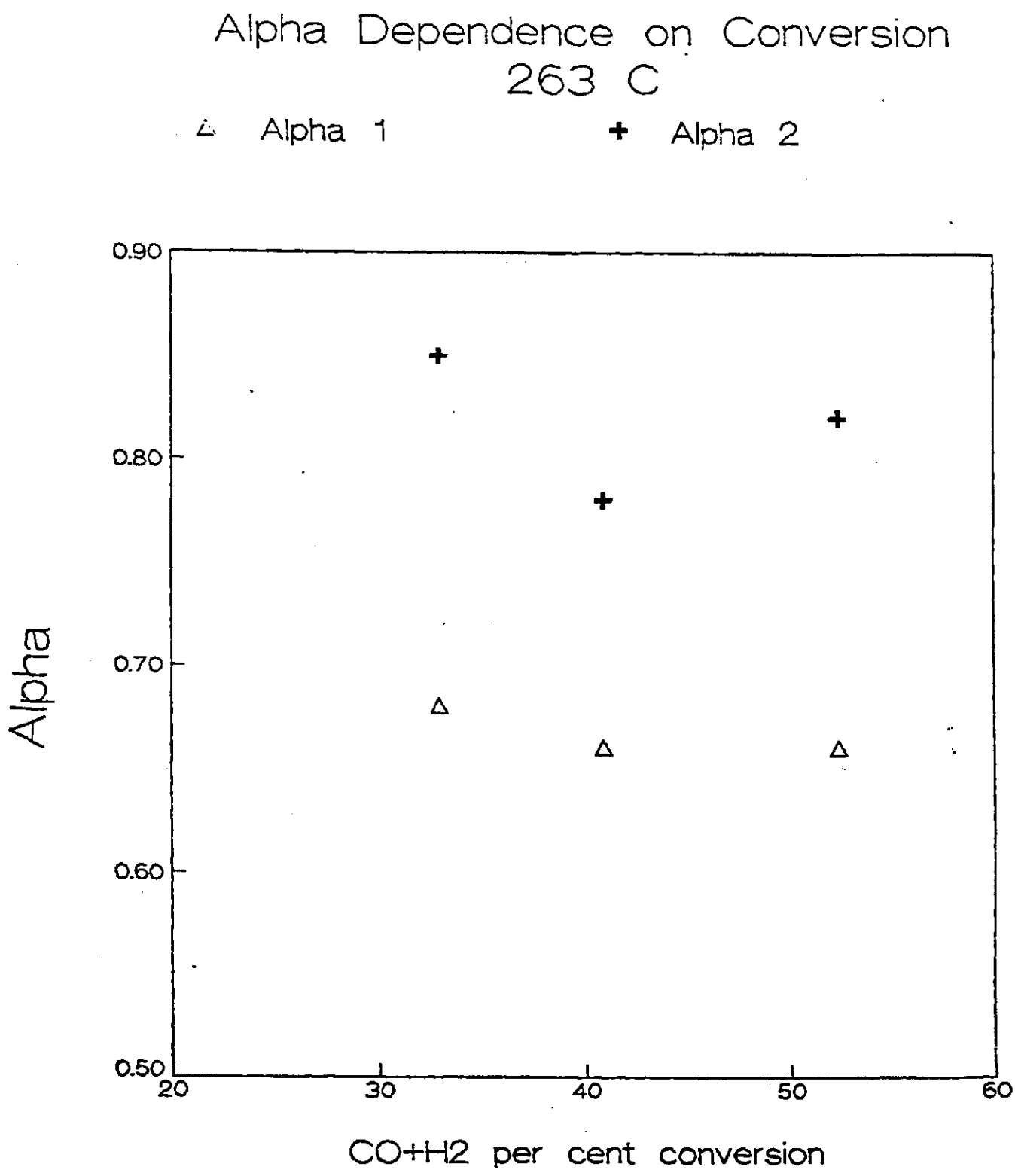
Alpha Dependence on Conversion
263 C
Alpha 1
Alpha 2
0.90
0.80
0.70
0.60
0.50
Alpha
20
30
40
50
60
CO+H2 per cent conversion

Figure 5

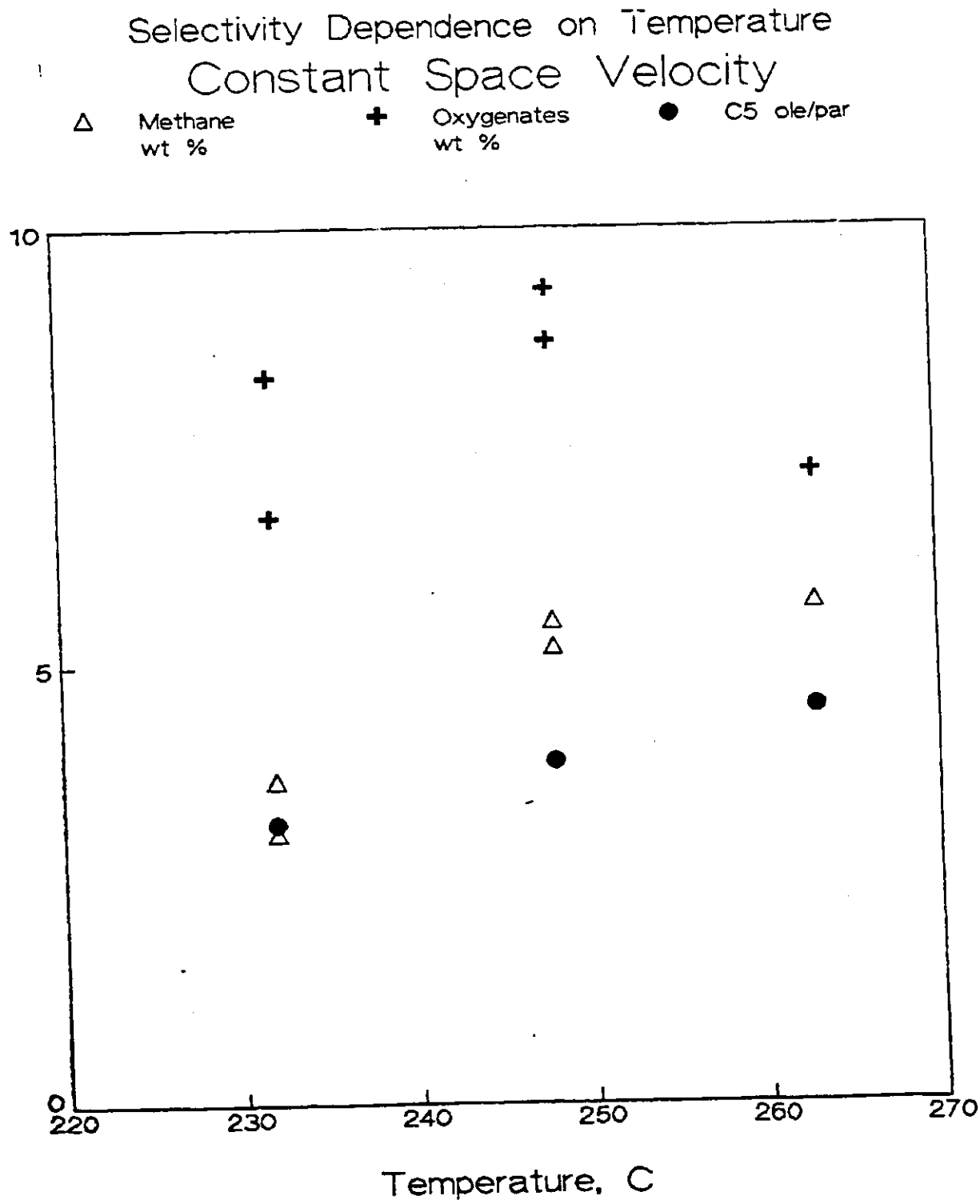
Selectivity Dependence on Temperature
Constant Space Velocity
Methane wt %
Oxygenates wt %
C5 ole/par
10
5
0
220
230
240
250
260
270
Temperature, C

Figure 6

Selectivity Dependence on Conversion

263 C

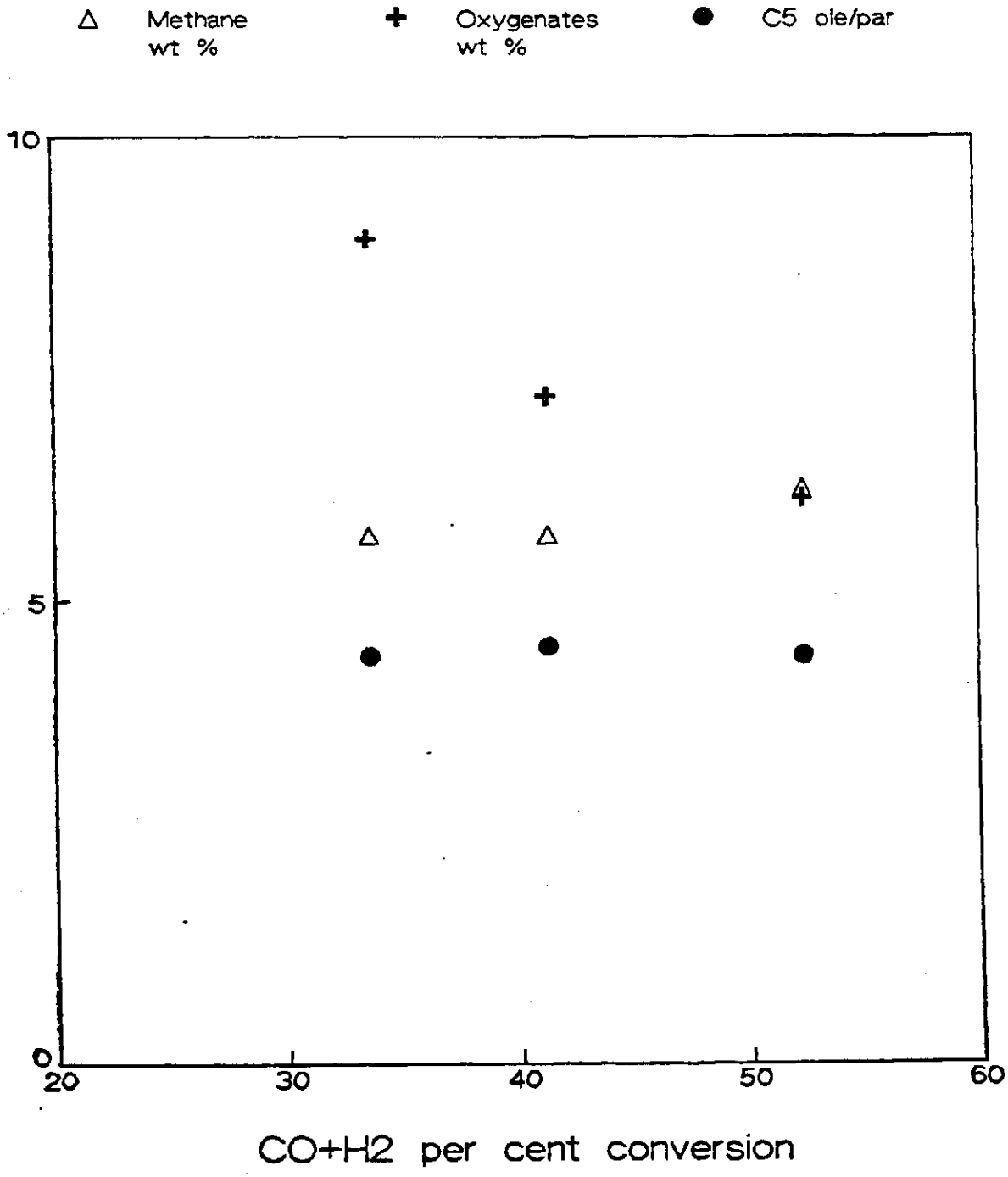

II. Effect of Added CO_2 on the Fischer-Tropsch Synthesis

1. A series of runs has now been completed, for the sets of conditions shown on Table 1.

Table I: Table of Runs (not chronological)

Syngas flow(l/min)	T(C)	P(psig)	% added CO2 to feed
0.4	232	100	0
0.4	232	123	20
0.4	232	214	50
0.8	232	100	0
0.8	232	123	20
0.8	232	214	50
1.3	232	100	0
1.3	232	123	20
0.8	263	100	0
0.8	263	123	20
0.8	263	214	50
1.3	263	100	0
1.3	263	123	20
1.3	263	214	50

Results are shown in Table 2.

Table II: Data from Run Fe 44

M.B.	T(°C)	P(atm)	Inlet Syn Flow (l/m)	p_{H_2} in (atm. abs.)	p_{CO}	p_{H_2O}	p_{CO_2}	X_{H_2}	X_{CO}	X_{CO+H_2}	$-R_{H_2+CO}$ (umol/min)
26	232	7.80735	0.399	2.31234	2.36927	0.05636	2.44782	55.0399	68.16	62.8	11.165
13	232	7.80143	0.405	2.19745	2.09881	0.065079	2.80432	62.17	73.95	69.0099	12.47
20	232	15.5756	0.407	1.66042	1.95848	0.11244	11.5203	55.77	86.99	58.96	10.703
16	232	9.51182	0.41	1.91867	1.89958	0.064989	5.08959	63.06	80.66	68.67	12.557
28	232	14.9524	0.79	2.06189	2.89196	0.16068	9.71563	38.14	79.49	38.17	13.4526
14	232	7.80998	0.887	2.76077	3.35877	0.03243	1.35058	38.78	45.84	42.87	16.964
17	232	9.51182	0.893	2.53236	3.1377	0.06062	3.50254	39.49	60.95	42.28	16.8459
15	232	7.80735	1.37	2.95266	3.71711	0.05296	0.87871	28.35	34.41	31.86	19.473
18	232	9.50919	1.372	2.69535	3.56979	0.065729	2.99178	29.64	52.23	30.83	18.867
23	263	15.566	0.779	1.29674	1.35217	0.20817	12.1742	67.22	91.5399	71.77	24.9409
25	263	7.80538	0.826	1.65418	0.98936	0.07665	3.97841	73.75	89.1499	82.86	30.535
11	263	9.77885	0.88	1.4513	1.11067	0.10584	6.31264	73.33	89.58	80.1799	31.462
8	263	7.80472	0.927	1.74456	1.12304	0.10874	3.82779	74.2599	87.95	82.19	33.992
24	263	15.5677	1.245	1.6824	1.9294	0.20463	11.2264	61.88	88.6	66.56	36.978
12	263	9.85285	1.368	1.81985	1.79531	0.070599	5.52061	64.36	82.21	70.19	42.8329
9	263	7.8034	1.38	2.13963	1.93518	0.03929	2.94111	63.2	75.7899	70.49	43.399

2. Experimental.

The slurry reactor was operated at 232°C and 263°C with C-73 catalyst. The pressure was varied between 0.79 MPa (100 psig) and 1.48 MPa (200 psig) and flow between 0.6 and 3.6 Ml/h/gFe.

Material balances were conducted with 0 mole %, ~20 mole % and ~50 mole % CO_2 added to the synthesis gas feed which had a H_2/CO ratio between 0.67 and 0.72. To avoid sampling during transient reactor conditions, the reactor was allowed 24 hours to achieve steady state following a feed or pressure change and 48 hours following a temperature change. When CO_2 was added to the feed the total reactor pressure was increased in such a way as to hold the inlet dry synthesis pressure constant. This was done to avoid observing dilution effects.

Material balances were required to have a 97-103% closure on oxygen. Returning to a given set of conditions periodically during the run indicated no significant loss in activity.

3. Kinetic Analysis.

Three kinetic models are shown in Table 3.

Table 3. Kinetic Models for Fischer-Tropsch Synthesis

Rate $-R_{CO+H2}$	Reference	Model
$apH_2pCO/(pH_2O + bpCO)$	Anderson (1956)	
$abpCOpH_2^2/(pH_2O + bpCOpH_2)$	Huff and Satterfield (1984)	A
$abpCOpH_2/(pCO_2 + bpCO)$	Deckwer, et al. (1986)	B

We are still analyzing the data, but it appears that when CO_2 is deliberately added, the effects observed are predominately caused by H_2O formed by the reverse water-gas shift, not by CO_2 as such.

Thus, the kinetic data follow the Huff kinetic expression, not that of Deckwer (see parity plot, Figure B, applying the Huff kinetics).

Without added CO_2, and with low H_2/CO feed, the water concentration is very low and the Deckwer correlation can be

applied (see Figure A). We are going to see if we can develop a new suitable model that will incorporate terms for both CO_2 and H_2O.

4. Selectivity.

A. Water-Gas-Shift Selectivity.

Figure C shows the effect of CO_2 on the ratio of rate of formation of H_2O to the rate of disappearance of CO. This is a measure of the extent of reverse water-gas-shift reaction which is seen to increase with p_{CO_2}. Therefore, at a given synthesis gas conversion, adding CO_2 increases p_{H_2O} and decreases p_{H_2} and, to a lesser extent, p_{CO}. It is important to keep these effects in mind when looking at the product selectivity changes that occurred upon addition of CO_2 to the feed.

B. Olefin/Paraffin Ratio.

In Figure D, the effect of CO_2 on the olefin $(\alpha+\beta)$/n-paraffin ratio for two carbon species at two temperatures is shown. At a given synthesis gas space velocity, an increase in CO_2 concentration increases the olefin/paraffin ratio. This relationship depends on conversion implying that olefin hydrogenation is a function of H_2 partial pressure rather than CO_2. The effect of CO_2 can largely be explained in terms of its effect on H_2 rather than by a more complex competitive adsorption mechanism. The effect of CO_2 on the rate of n-butane and n-pentane formation divided by H_2 partial pressure is shown in Figure E. At low temperature, CO_2 has no apparent effect on the rate of paraffin formation. At high temperature, the data are scattered and the hydrogenation rate seems to depend on more than

the H_2 partial pressure. It is conceivable that at high temperatures the rate expression is more complicated. However, it appears that CO_2 inhibition is not a factor.

C. Oxygenate Selectivity.

In Figure F, the mole fraction of oxygenated compounds formed at C_2 and C_4 is seen to increase slightly with CO_2 partial pressure at a given synthesis gas space velocity. This oxygenate selectivity trend depended on synthesis gas conversion. As CO_2 was added to the feed at a given synthesis gas space velocity, greater amounts of H_2O were observed. As detailed above, this increase in H_2O was due primarily to the reverse water-gas-shift reaction. As reported by Hanlon and Satterfield (1984), an increase in the H_2O concentration increases the production of oxygenates at a given carbon number. Figure G is a plot of the same oxyygenate selectivity data against H2O partial pressure. The effect of CO_2 is to increase the concentration of H_2O which has been shown to increase the selectivity to oxygenates.

D. Methane Selectivity.

In Figures H and I, methane selectivity, defined as the molar ratio of methane to C_1-C_6 fraction, is shown as a function of CO_2. At fixed tmperature and synthesis gas space velocity, methane selectivity decreased with increasing CO_2. However, this change in methane selectivity can be explained solely by changes in H_2 concentrations. Figure J shows the rate of methane formation as a function of p_{H_2}. Methane formation appears to be first order in H_2 at all CO_2 concentrations.

FIGURE A

CO2 Inhibition of Rate

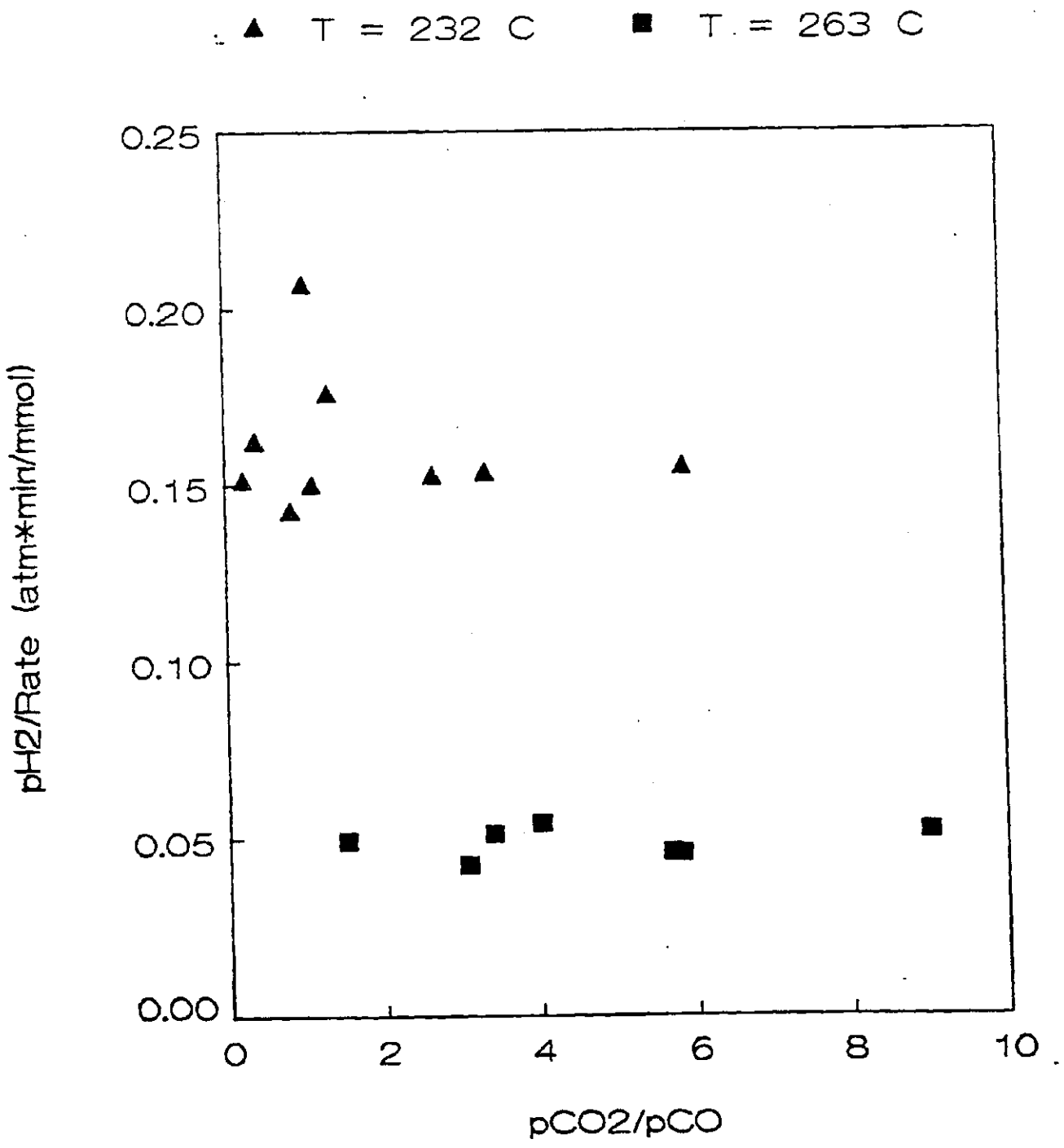

FIGURE B

Experimental and Predicted Rate

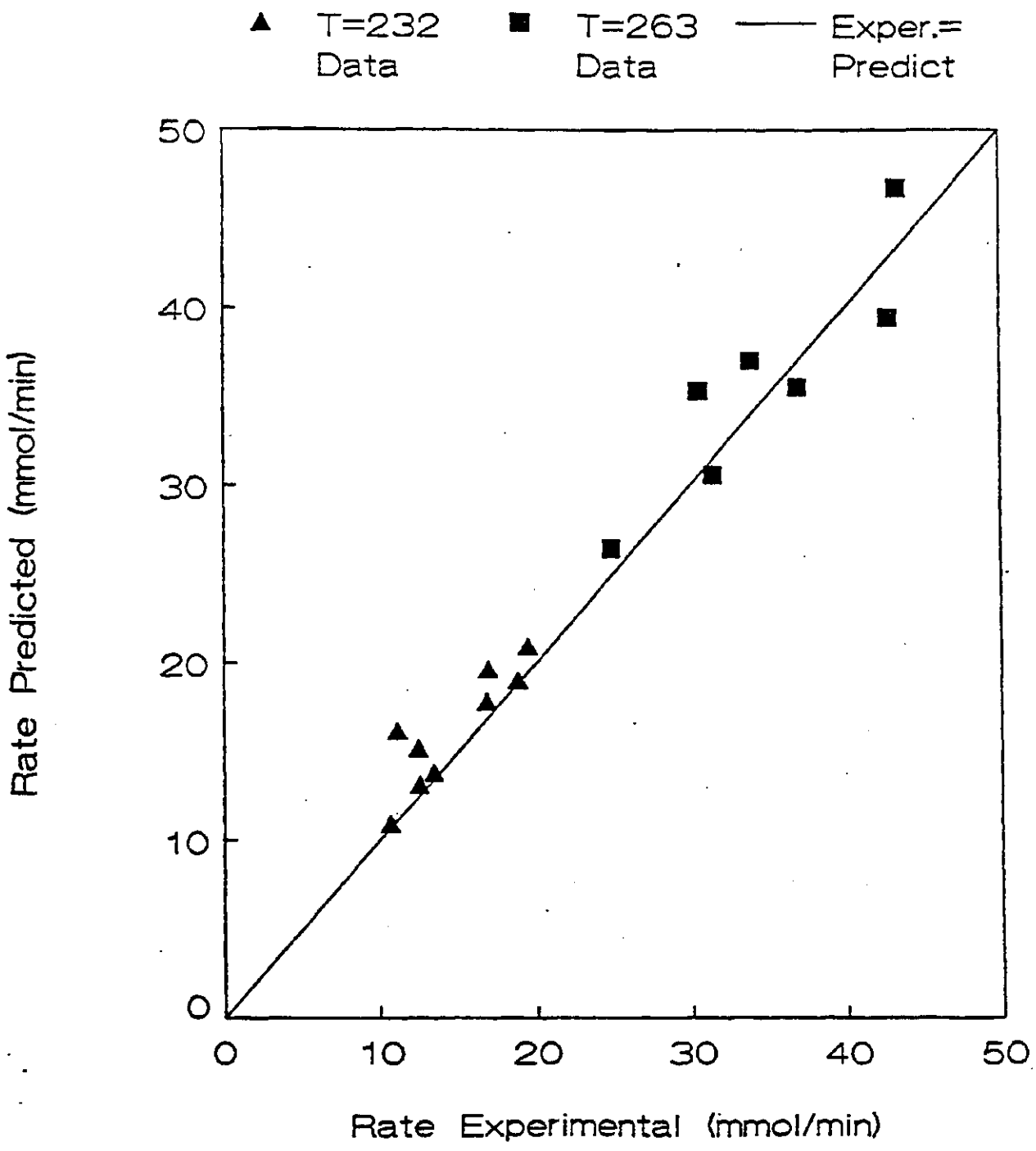

FIGURE C

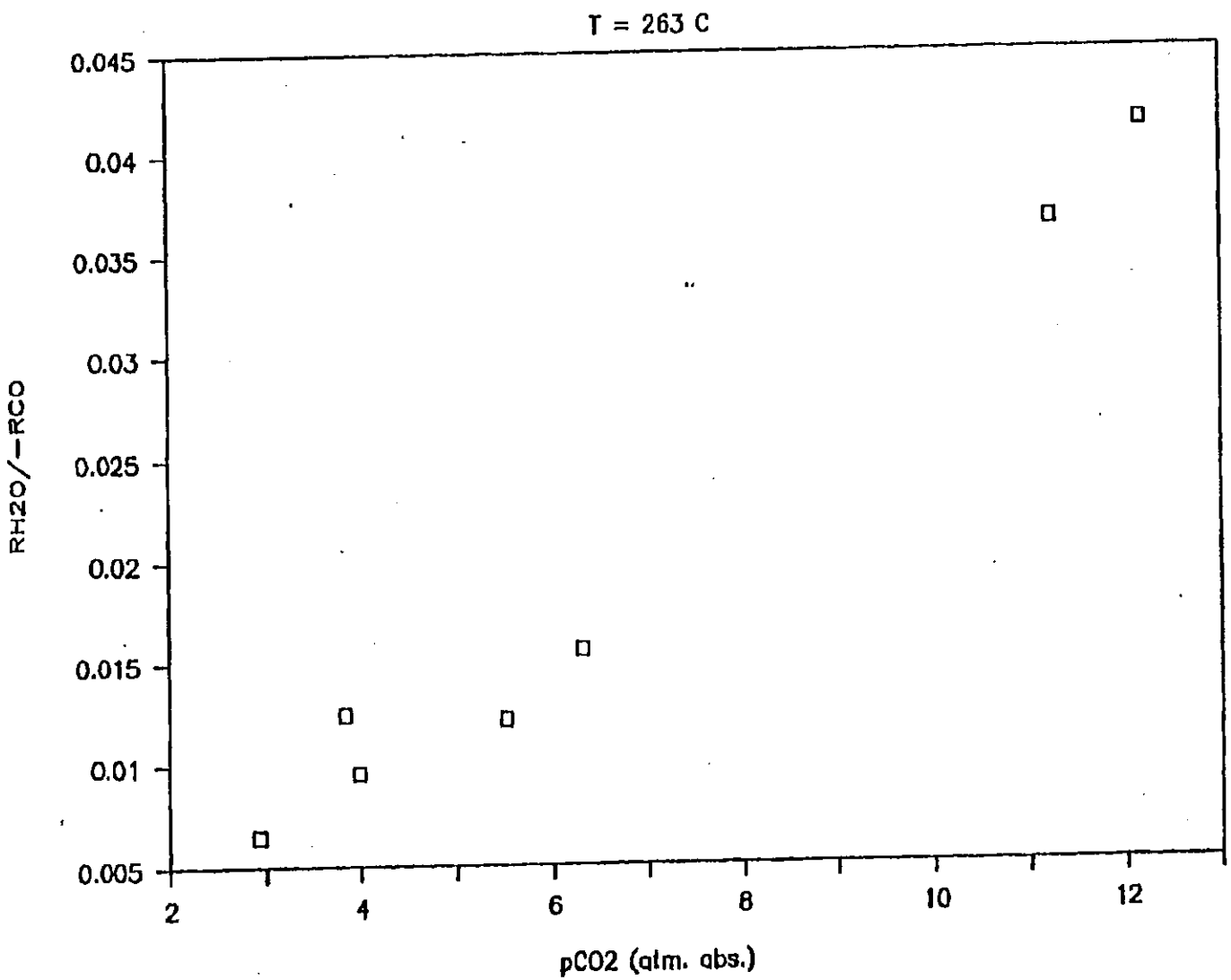
Effect of CO2 on WGS Selectivity
T = 263 C
0.045
0.04
0.035
0.03
0.025
0.02
0.015
0.01
0.005
RH2O/-RCO
2
4
6
8
10
12
pCO2 (atm. abs.)

FIGURE D

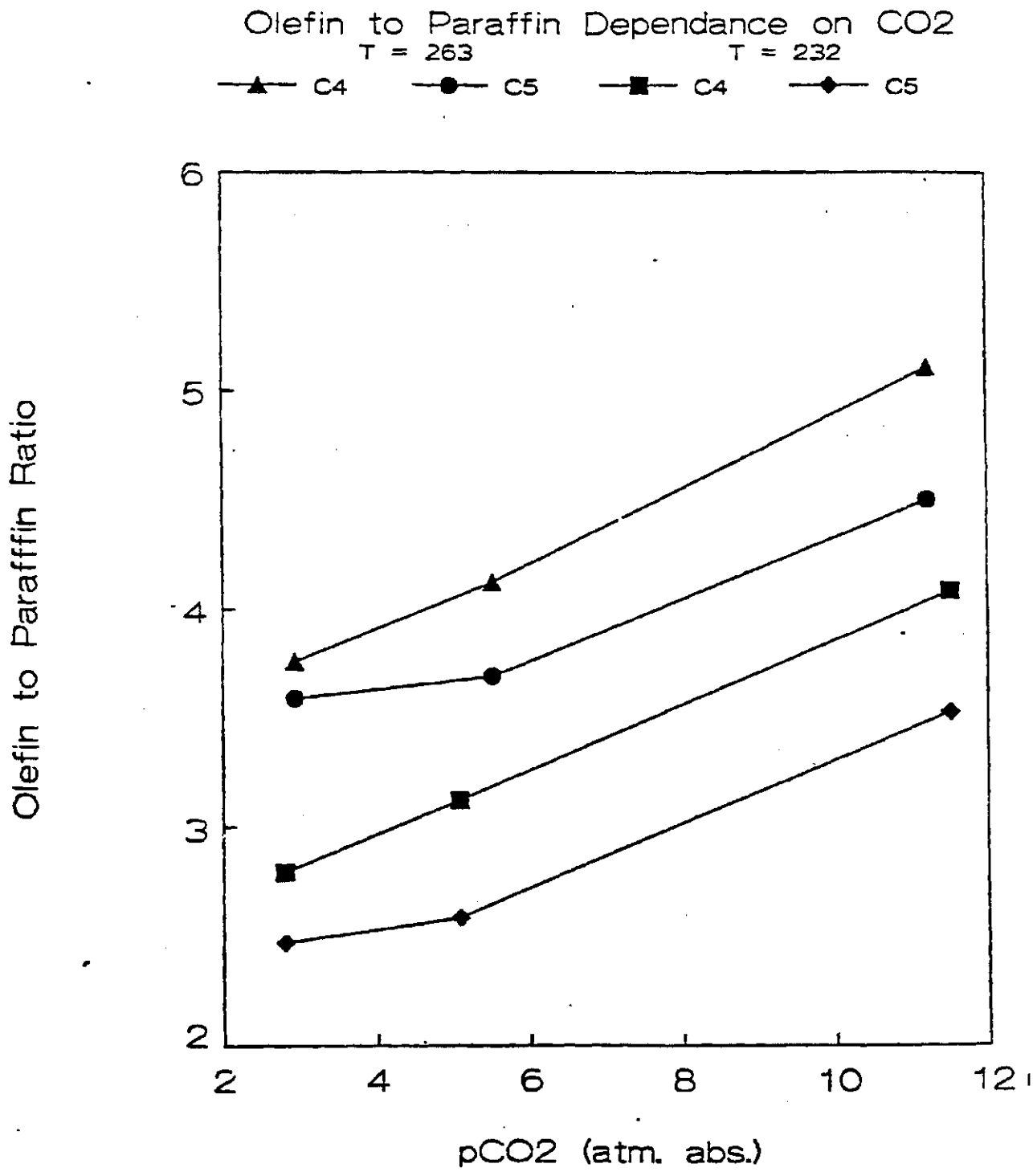
Olefin to Paraffin Dependance on CO2
T = 263
T = 232
C4
C5
C4
C5
Olefin to Parafffin Ratio
6
5
4
3
2
2
4
6
8
10
12
pCO2 (atm. abs.)

FIGURE E

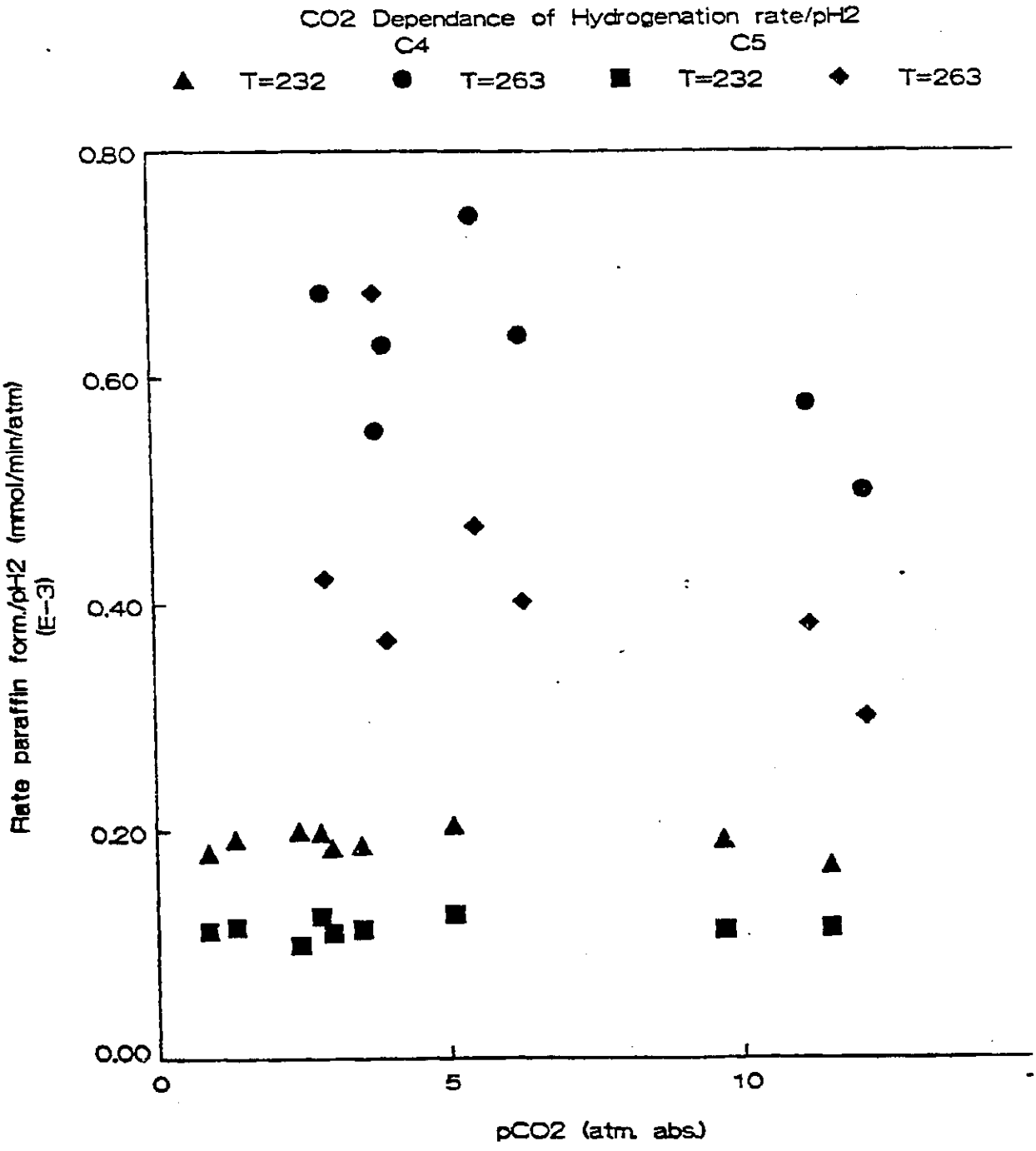
CO2 Dependance of Hydrogenation rate/pH2
C4
C5
T=232
T=263
T=232
T=263
0.80
0.60
0.40
0.20
0.00
Rate paraffin form./pH2 (mmol/min/atm) (E-3)
0
5
10
pCO2 (atm. abs.)

FIGURE F

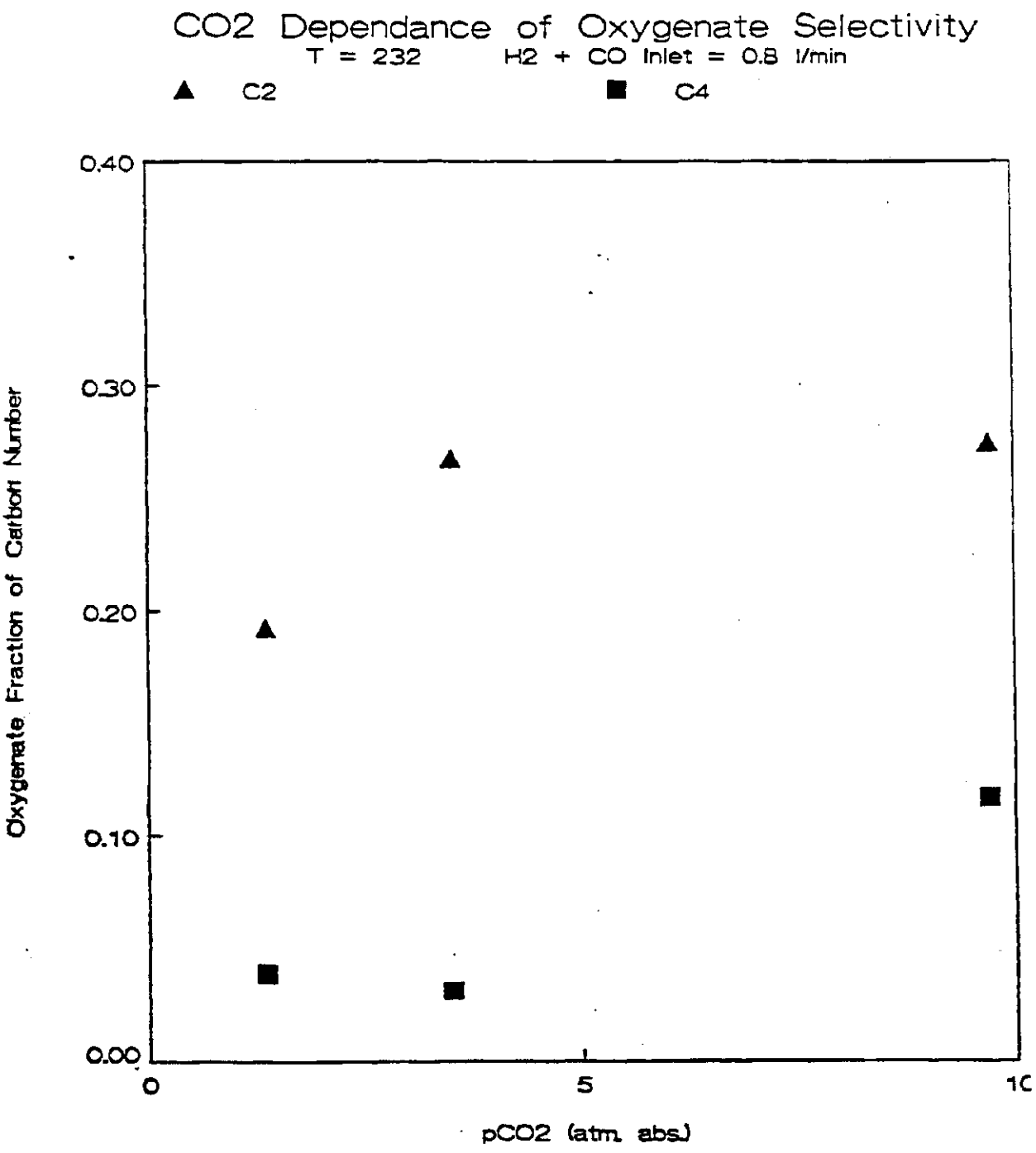
CO2 Dependance of Oxygenate Selectivity
T = 232 H2 + CO Inlet = 0.8 l/min
C2
C4
0.40
0.30
0.20
0.10
0.00
Oxygenate Fraction of Carbon Number
0
5
10
pCO2 (atm. abs.)

FIGURE G

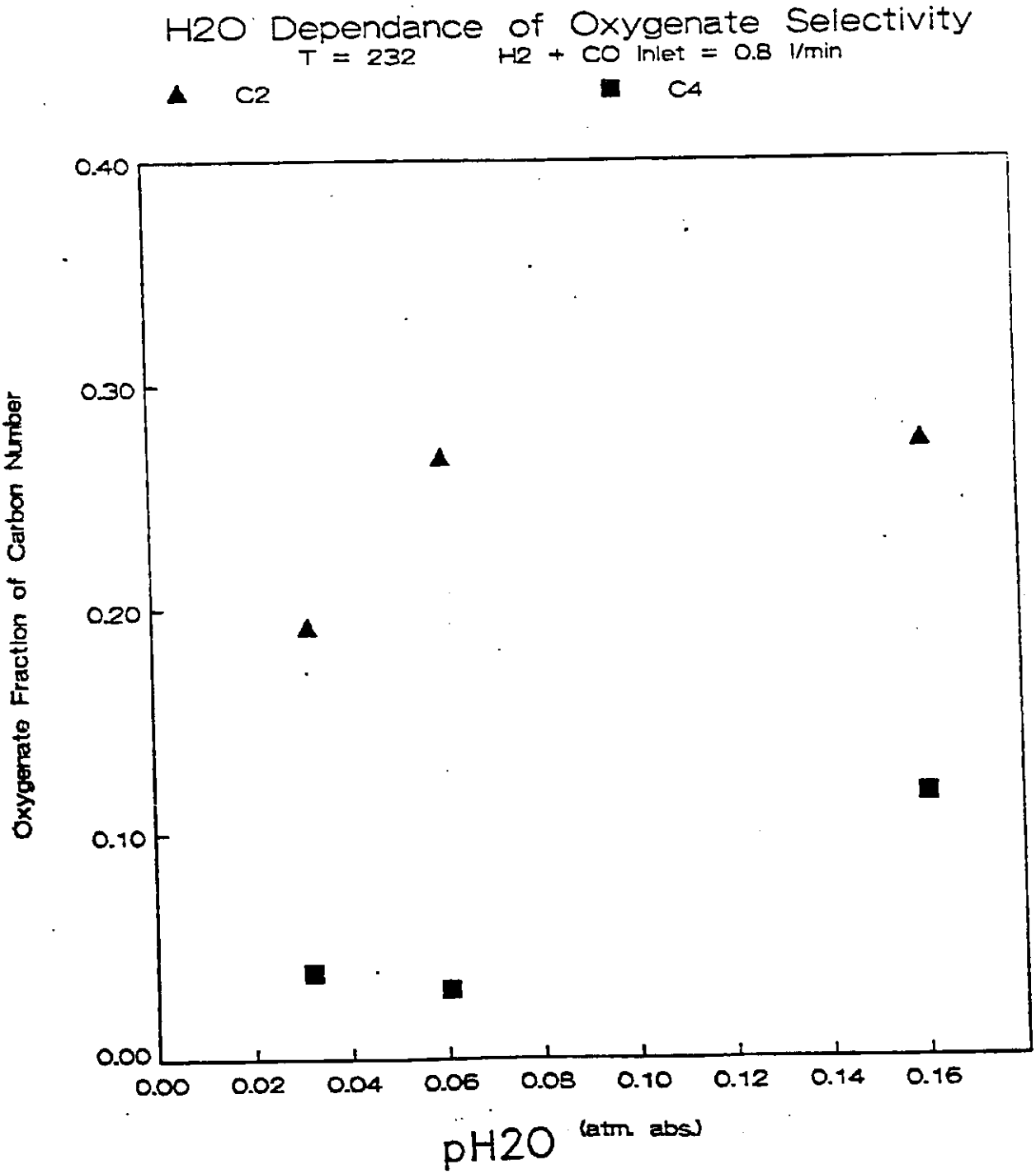
H2O Dependance of Oxygenate Selectivity
T = 232 H2 + CO Inlet = 0.8 l/min
C2
C4
Oxygenate Fraction of Carbon Number
0.40
0.30
0.20
0.10
0.00
0.00
0.02
0.04
0.06
0.08
0.10
0.12
0.14
0.16
pH2O (atm. abs.)

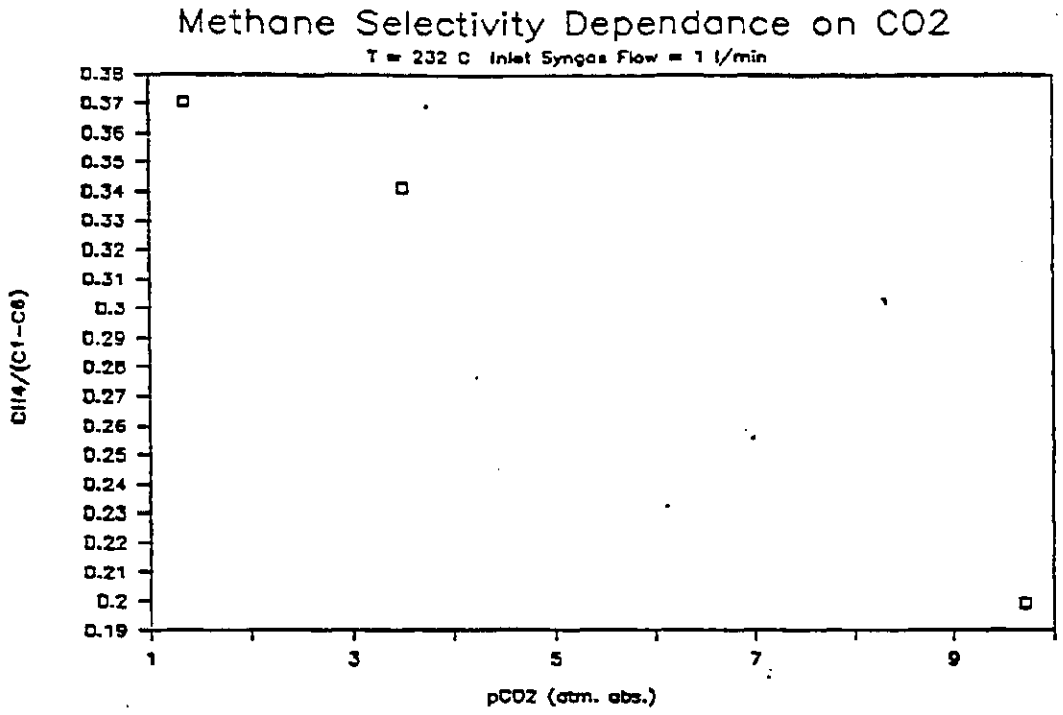

FIGURE H

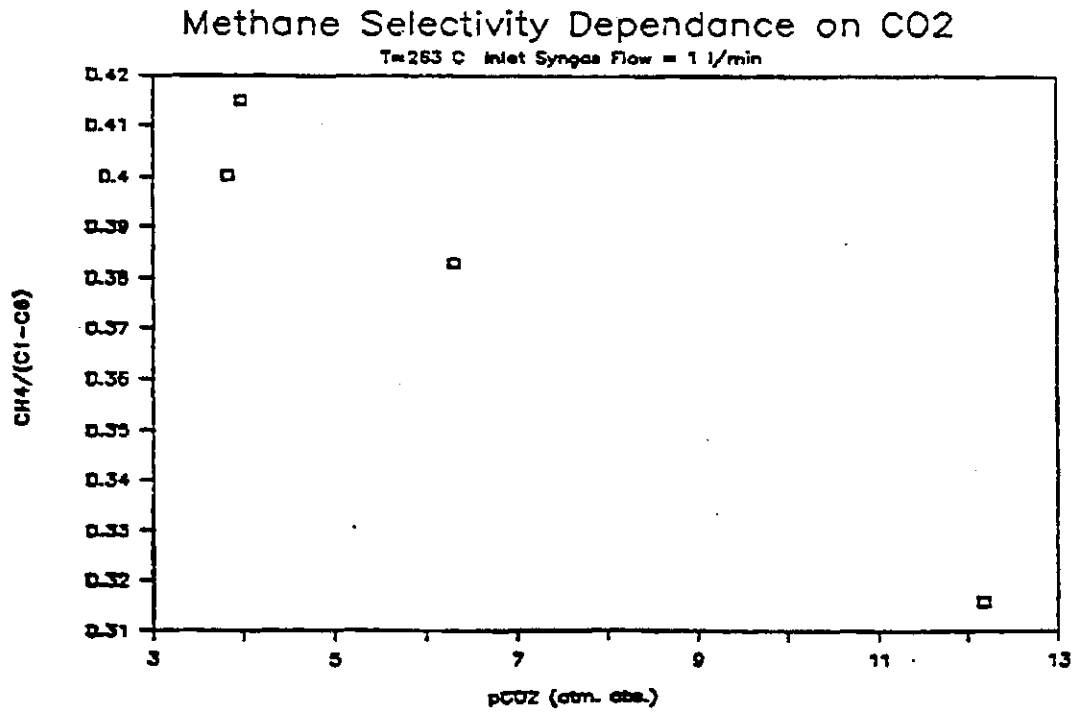

FIGURE I

FIGURE J

Methane Formation Dependance on H2